

Searching for light dark matter with the PADME experiment

Isabella Oceano^{a,b,*} and on behalf of PADME collaboration[§].

^a*Dipartimento di matematica e fisica, Università del Salento,
Lecce, Italy*

^b*INFN Lecce
Lecce, Italy*

E-mail: isabella.oceano@le.infn.it, isabella.oceano@gmail.com

The search for dark matter at accelerators has gained a lot of attention in recent years. Among the theoretical scenarios that can be studied, an attractive one is postulating a new $U_D(1)$ gauge symmetry mediated by a massive boson often named dark photon A' . The A' could be the bridge between the Standard Model (SM) and a hypothetical Dark Sector (DM), having a small coupling ϵ with SM particles. PADME (Positron Annihilation to Dark Matter Experiment) is the first fixed target experiment searching for the A' produced in association with a photon in e^+e^- annihilations. It exploits the missing mass technique and does not make any assumption on the decay mode of the A' . PADME is located at the Laboratori Nazionali di Frascati (LNF) of INFN and it is designed to be sensitive to the production of a dark photon with mass $M'_A \leq 23.7$ MeV. Its setup is also ideal to investigate other scenarios of low mass dark matter: axion-like particles (ALPs), dark Higgs, and the X_{17} boson claimed to explain anomalies observed recently in a nuclear physics experiment.

*Corfu Summer Institute 2021 "School and Workshops on Elementary Particle Physics and Gravity"
29 August - 9 October 2021
Corfu, Greece*

[§]A.P. Caricato, M. Martino, I. Oceano, S. Spagnolo (INFN Lecce and Salento Univ.), G. Chiodini (INFN Lecce), F. Bossi, R. De Sangro, C. Di Giulio, D. Domenici, G. Finocchiaro, L.G. Foggetta, M. Garattini, A. Ghigo, P. Gianotti, I. Sarra, T. Spadaro, E. Spiriti, C. Taruggi, E. Vilucchi (INFN Laboratori Nazionali di Frascati), V. Kozhuharov (Sofia Univ. "St. Kl. Ohridski" and INFN Laboratori Nazionali di Frascati), S. Ivanov, Sv. Ivanov, R. Simeonov (Sofia Univ. "St. Kl. Ohridski"), G. Georgiev (Sofia Univ. "St. Kl. Ohridski" and INRNE Bulgarian Academy of Science), F. Ferrarotto, E. Leonardi, P. Valente, A. Variola (INFN Roma1), E. Long, G.C. Organtini, G. Piperno, M. Raggi (INFN Roma1 and "Sapienza" Univ. Roma), S. Fiore (ENEA Frascati and INFN Roma1), V. Capirossi, F. Iazzi, F. Pinna (Politecnico of Torino and INFN Torino), A. Frankenthal (Princeton University)

*Speaker

1. The dark photon theory

Gravitational anomalies observed in the universe have led to a growing awareness of the existence of dark matter, although deep studies need to be accomplished to understand its characteristics. Hence, the investigation of dark matter nature, its origin, and the way it interacts with ordinary matter plays a crucial role today in fundamental science. One of the models that has received particular attention from the scientific community in recent years is the WIMP model, which involves a dark matter candidate at the electroweak scale. However, no evidence of the validity of this approach has been obtained up to now. It is for this reason that other models need to be investigated. One intriguing hypothesis postulates dark matter constituents being neutral under Standard Model interactions. The interaction between the two sectors is realized through a new, still unknown, force due to an “hidden” charge. The new symmetry $U_D(1)$ is mediated by a massive Abelian gauge boson A' , the dark photon. A' might play the role of a neutral vector portal connecting the visible and the dark sector. It can interact weakly with the SM particles by means of a Lagrangian term:

$$L_{int} = \frac{\epsilon}{2} F_{\mu\nu}^D F_{SM}^{\mu\nu} \quad (1)$$

where ϵ is an effective coupling parameter that can be small enough to preclude the discovery of the dark photon in many experiments. Besides ϵ , the only parameter of this model is the mass $m_{A'}$ of the dark photon. This term breaks the gauge invariance of the dark interactions and can be generated through different mechanisms [1]: Stückelberg mechanism, introducing an interaction term of A' with a scalar with the form:

$$L_{mass} \sim \frac{1}{2} (\partial^\mu \alpha + m A'^\mu) (\partial_\mu \alpha + m A'_\mu). \quad (2)$$

Imposing unitarity conservation, this leads to a mass term corresponding to a spin-1 field; furthermore the mass term can derive from an additional scalar field charged under $U_D(1)$, the “dark Higgs”. The additional terms to the “dark” Lagrangian, after spontaneous symmetry breaking, would be:

$$L_{mass} \sim \frac{1}{2} m_{A'}^2 A'_\mu A'^\mu + g' m_{A'} h' A'_\mu A'^\mu + \frac{1}{2} g'^2 h'^2 A'^2 \quad (3)$$

where h' is the dark Higgs field and g' is the $U_D(1)$ coupling constant; the last mass generation mechanism occurs through the interaction of A' with the Standard Model Higgs [2].

The production mechanisms foreseen for A' are various and can be categorized as follows:

- Bremsstrahlung, or A' -strahlung on nuclei, $e^\pm N \rightarrow e^\pm N A'$: dark photon production in lepton-on-target processes;
- Annihilation process, of positrons with electrons, $e^+ e^- \rightarrow \gamma A'$: dark photon production in lepton-on-target processes;
- Decays of neutral mesons such as π^0 , η , ϕ e Υ . Mesons may be produced in fixed target experiments, $e^+ e^-$ colliders or jets in hadron colliders;
- Drell-Yan (DY) process, $q\bar{q} \rightarrow A' \rightarrow l^+ l^-, h^+ h^-$ at hadron colliders and at fixed target experiments with proton beam.

The decay mode of the new particle depends on the mass hierarchy of the dark sector, and three scenarios are possible. If the mass of any dark particle χ satisfies the relation $2m_\chi > m_{A'}$, the dark photon will decay through SM particles (visible decay) with a branching ratio $\Gamma \propto \epsilon^2$ and if $m_{A'} < 2m_\mu$ the only final state accessible is $A' \rightarrow e^+e^-$. Otherwise, if $m_{A'} > 2m_\chi$ the main decay mode will be $A' \rightarrow \chi\chi$ (invisible decay) not suppressed by the ϵ factor. The experimental methods used to search for dark photon decay are developed based on this mass hierarchy. When studying visible decay, the experiments exploit two characteristics of the dark photon: mass and decay time. Under the assumption $m_{A'} > 2m_\chi$, a large region of the space parameters is still unexplored. In this case, the branching ratio for the visible decays of A' is strongly suppressed since the coupling between SM particles and A' is very weak. To detect dark photon decays in DM particles, new search techniques have to be used. In detail, missing mass, momentum, and energy studies can be exploited.

The search for a massive dark photon has been pursued with large enthusiasm in the latest years and many experiments re-interpreted their data to probe this hypothesis. The strategies adopted to probe the A' hypothesis depend on the dark photon decay mode: visible or invisible. The limits for visible and invisible decay are reported in Figure 1.

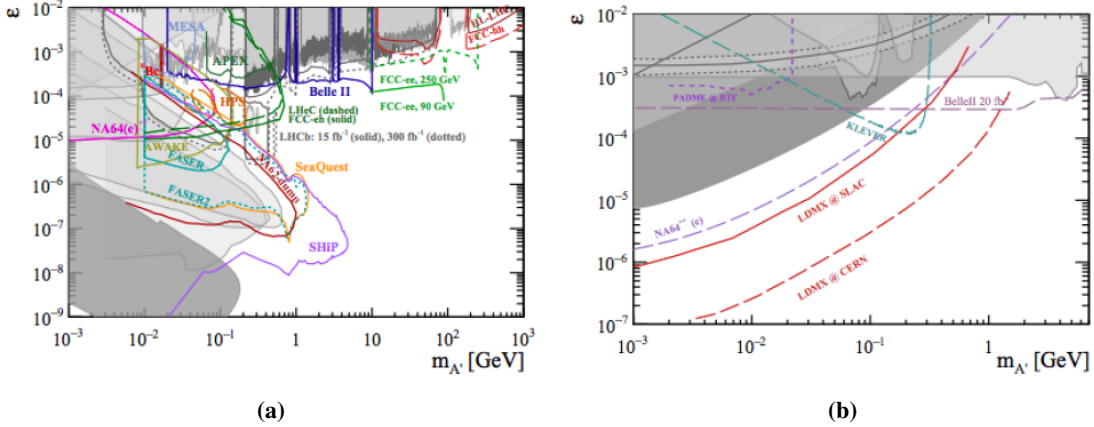


Figure 1: Perspectives in terms of exclusion regions in the space parameters $(M'_{A'}, \epsilon)$ for visible (a) and invisible (b) decays of the dark photon from several forthcoming experiments [3].

2. The PADME experiment

The PADME experiment is designed to probe the dark photon hypothesis in the invisible decay channel. In the experiment, the A' production happens via the annihilation process $e^+e^- \rightarrow \gamma A'$, and the method used for its detection is the missing mass, thus a peak in the $M_{miss}^2 = (p_{e^+} + p_{e^-} - p_\gamma)^2$ distribution will be the signature of the existence of the dark boson.

PADME is a INFN project approved in 2016 and installed in 2018 at the Laboratori Nazionali di Frascati. The LINAC of DAΦNE [4] provides a positron beam with $E_{e^+} \leq 550$ MeV. Since the production happens via positron-electron annihilation, the maximum value of $m_{A'}$ that PADME can reach is $m_{A'} \leq \sqrt{2m_e E_{e^+}} = 23.7$ MeV. Figure 2 shows a schematic picture of the experiment.

Entering from the left, the beam hits an active target, made of CVD Diamond [5] [6], then a region follows where the particles propagate inside a vacuum chamber placed in the gap of a magnetic dipole. The neutral particles produced in the e^+e^- interaction reach a calorimeter system placed in the forward direction, consisting of the main calorimeter (ECAL) [7] and the Small Angle Calorimeter (SAC) [8]. ECAL consists of 616 BGO crystals arranged in a cylindrical matrix with a $5 \times 5 \text{ cm}^2$ central squared hole. Its main purpose is to detect the ordinary photon produced in association with the A' . The SAC calorimeter is installed behind the central hole of ECAL calorimeter. It consists of a 5×5 matrix of PbF_2 Cherenkov crystals and provides fast detection and rejection of forwarding photons from Bremsstrahlung of the positron beam on the target. The detection of charged particles is performed by means of a veto system. It is located inside the PADME vacuum vessel and consists of three stations of plastics scintillators (EVeto for e^- , PVeto for e^+ and HEPVeto for high energy e^+) [9].

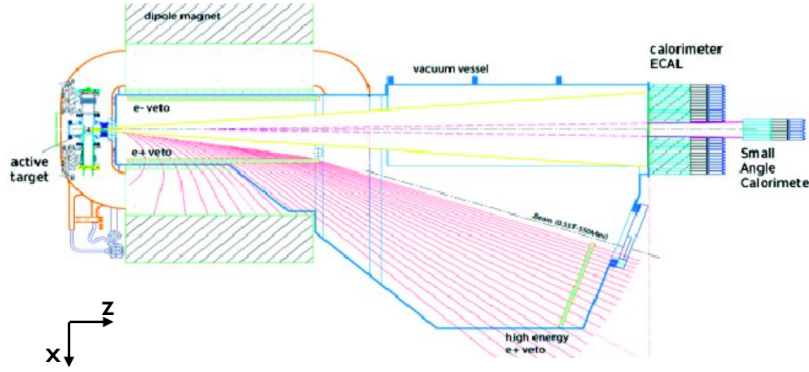


Figure 2: Layout of the PADME experiment (top view).

3. Backgrounds processes in PADME

The most dangerous background, in the A' search, is represented by positron Bremsstrahlung, due to the high cross-section and the presence of a single photon in the final state that mimics the signal. The positron Bremsstrahlung cross-section at leading order was evaluated using Geant4 [12] and turned out to be of the order of $\sigma(e^+N \rightarrow e^+N\gamma) \simeq 4 \text{ b}$ for positron energy of 550 MeV and producing a photon of energy above 1 MeV. Bremsstrahlung photons are produced mainly in the forward direction, for these events the geometrical acceptance of PADME is very close to 1. The same is true for the radiative Bhabha $e^+e^- \rightarrow e^+e^-\gamma$, which cross-section is extracted at leading order using CalcHEP [11] and it is equal to $\simeq 180 \text{ mb}$ for $E_\gamma > 1 \text{ MeV}$. In PADME, these events can be identified by checking the presence of a positron in the PVeto or in the HEPVeto and a photon in the calorimeter system. In case of absence of a track in the positron vetoes, the event has the same signature as the dark photon event. These events give entries at high values on the squared missing mass spectrum, as Figure 3 shows.

Another SM process that can mimic the signal, is the annihilation into two or three photons $e^+e^- \rightarrow \gamma\gamma(\gamma)$. The leading order cross-section of the annihilation $e^+e^- \rightarrow \gamma\gamma$ is given by the

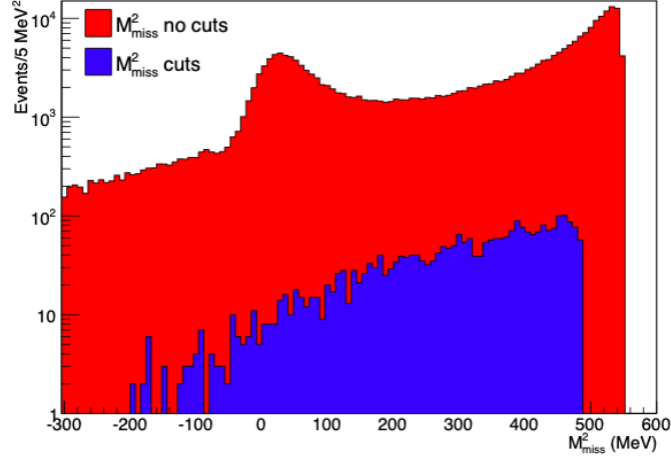


Figure 3: M_{miss}^2 distribution for background events before (red) and after selection cuts applied (blue) [10]. The details of the applied cuts are given in the text.

Heitler formula:

$$\sigma(E, Z) = \frac{Z\pi r_e^2}{\gamma + 1} \times \left[\frac{\gamma^2 + 4\gamma + 1}{\gamma^2 - 1} \ln(\gamma + \sqrt{\gamma^2 - 1}) - \frac{\gamma + 3}{\sqrt{\gamma^2 - 1}} \right] \quad (4)$$

where E is the positron energy, r_e is the classical electron radius and γ is the Lorentz factor of the positron. The leading order cross section, for a beam energy of $E_{beam} = 550$ MeV, obtained with Equation 4 is in agreement with CalcHEP calculation: $\sigma(e^+e^- \rightarrow \gamma\gamma) = 1.55$ mb. In PADME, this process is identified by the presence of two photons in the ECAL calorimeter. Using CalcHEP generated events and the MC code of the experiment, the geometrical acceptance α and the efficiency ϵ of the event reconstruction has been estimated to be of the order of $\alpha \times \epsilon \simeq 0.08$. The presence of a single photon in the calorimeter mimics the dark photon signature. These events, due to photon detection inefficiency, give entries at values of squared missing mass peaked to zero, as Figure 3 shows.

The last background for the dark photon search is the annihilation of three photons. Its cross-section, calculated using CalcHEP, is about $170 \mu\text{b}$, assuming $E_\gamma > 1$ MeV. A reliable value of the detector acceptance is not easy to be obtained without a proper generator, thus the yield of the three-photon annihilation process is not yet precisely determined in PADME. However, an estimation, obtained with CalcHEP setting $E_\gamma > 50$ MeV, gives a value $\sim 10 \mu\text{b}$. The three-photon final state can have the same signature of the dark photon if two photons do not enter in the acceptance of the calorimeter or in case of photon detection inefficiencies. A three-photon annihilation which results in the detection of just one photon gives entries in the squared missing mass spread in all the spectrum.

Table 1 reports the number of events expected in ECAL, for a standard day of data taking, together with the total cross-section and the acceptance corrected cross-section.

Table 1: Simulated total cross sections (σ) and daily production rates (N) of SM processes in PADME in standard run conditions ($\approx 28 \times 10^3$ POT/bunch corresponding to $N_{POT} = 1.11 \times 10^{11}$ /day,) are also reported. Acceptance corrected cross sections σ^* and daily production rates (N^*). The MC generators used are also indicated.

Process	σ [pb]	$N/10^{11}$ POT	σ^* [pb]	$N^*/10^{11}$ POT	Generator	E_{beam} [MeV]
$e^+N \rightarrow e^+N\gamma$	4E12	4.7E9	4E12	$\approx 1E9$	Geant4	500
$e^+e^- \rightarrow e^+e^-\gamma$	0.18E12	2.1E8	0.131E9	1.5E5	CalcHEP	550
$e^+e^- \rightarrow \gamma\gamma$	1.55E9	1.8E6	0.12E9	1.3E5	CalcHEP	550
$e^+e^- \rightarrow \gamma\gamma\gamma$	0.170E9	1.9E5	0.01E9	1.2E4	CalcHEP	550

4. PADME data taking

The installation of the PADME detector began in July 2018, and already on September 15th, the experiment started the commissioning data taking. PADME tested several beam configurations in order to understand the beam-induced background and the detectors occupancy. The first physical data taking took place from November 1st 2018 till March 1st 2019. Figure 4 (a) shows the integrated luminosity collected by PADME in this run. The total luminosity acquired by PADME during RunI was $L_{RunI} = (6.37 \pm 0.32_{sys}) \times 10^{12}$ POT. The data collected with different beam settings lead to the understanding of the source of backgrounds. In particular, using the positron converter close the PADME hall, the background level is higher by a factor of 10 than that obtained when the converting target is placed at the beginning of the beamline.

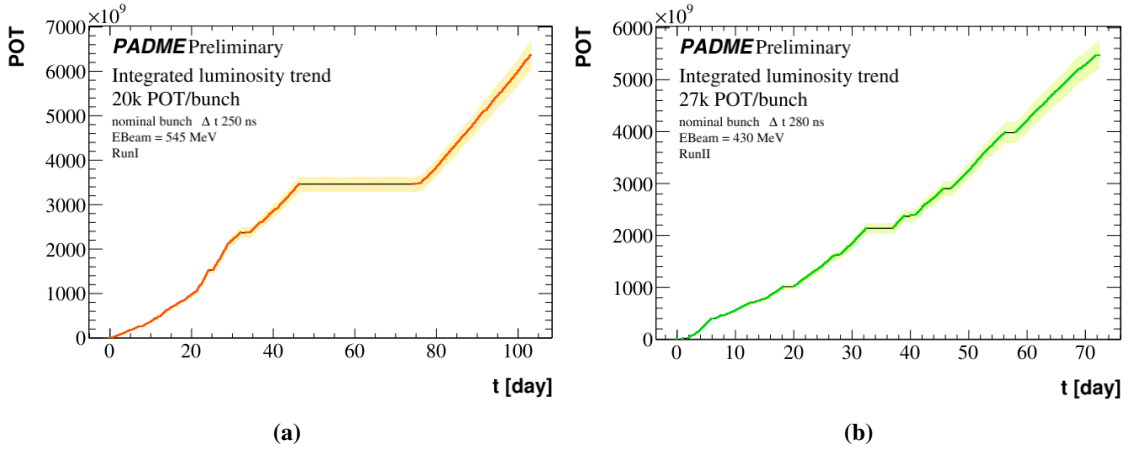


Figure 4: Integrated luminosity collected by PADME in RunI (a) and RunII (b). The orange/green curves represent the cumulative measurement of the POT (Positron On Target) as a function of the data-taking day; the yellow/light green bands show the systematic error of 5%.

After RunI, commissioning runs were taken during July 2019 both to study the beam-related background and to calibrate the detectors.

The RunII started in September 2020 and ended in December 2020, data were collected with a better beamline configuration, determining a lower background level in the detectors. Figure

4(b) shows the integrated luminosity of PADME for RunII. The total accumulated statistics is $L_{RunII} = (5.47 \pm (0.27)_{sys}) \times 10^{12}$ POT.

5. Detection of Standard Model processes in PADME

As described in Section 3, the main source of backgrounds in the experiment are the Bremsstrahlung and the annihilation in SM particles. Therefore, a big effort was put by the collaboration to improve the knowledge of these two processes. In this section, the results obtained analysing the best RunI data are reported.

5.1 Bremsstrahlung

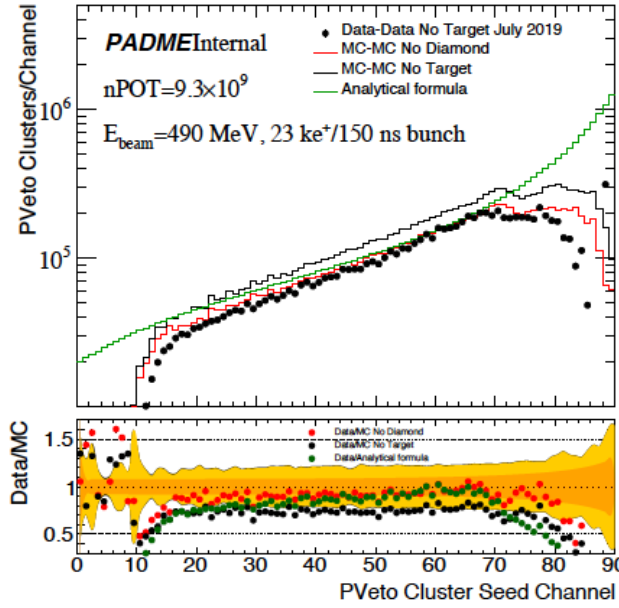


Figure 5: Bremsstrahlung yield profile in the PVeto as a function of the position along the z axis, expressed in terms of scintillator channel number, for data (black dots) and two MC sets (red and black solid line) superimposed with the spectrum obtain from the analytical formula (green solid line) [13] (see text for more details).

Figure 5 shows the distribution of the channel number of the PVeto cluster seed after the subtraction of the beam background component. This latter is estimated using special data collected removing the target from the beamline. The Bremsstrahlung yield profile measured was compared with MC simulated events. The simulated beam background was evaluated removing the diamond target with its board and aluminium support or removing the Diamond material only. In the plot, the black and red solid lines correspond to the Bremsstrahlung yield profile estimated subtracting the two background simulations. The analytical determination of the Bremsstrahlung in the diamond target in the complete screening approximation [14] is also reported in green.

From the comparison emerges that the simulation and the analytical prediction well describe the data in the channel range [40, 70]. Indeed, in this range the beam background, although high,

does not overwhelm the detector. The systematic uncertainties showed in Figure 5 by an orange band, are dominated by the modelling of the beam-related background, the momentum calibration, and the number of positrons collected on the target.

5.2 Annihilation

The two-photon annihilation is a very important SM candle process for PADME. Gaining a good knowledge of this interaction allows monitoring the energy scale, the number of positrons hitting the target, and verify detector geometry. In addition, it allows exercising on an easy test case the strategy to fight the background for the dark photon search. The signature of this process in the experiment consists in the detection of two photons in the electromagnetic calorimeters. Since the SAC detector is overwhelmed by Bremsstrahlung photons, only the main calorimeter, ECAL, is used to perform the analysis. The selection of annihilation processes is based on the constrained photon-photon kinematics. From this it is possible to assert that the sum of the energies $E_{\gamma_1} + E_{\gamma_2}$ is equal to the beam energy, furthermore the photons are back to back in the transverse plane and as a consequence the Center of Gravity of the two photons is close to zero:

$$x(y)_{CoG} = \frac{x(y)_1 E_{\gamma_1} + x(y)_2 E_{\gamma_2}}{E_{\gamma_1} + E_{\gamma_2}} \sim 0. \quad (5)$$

where $x(y)$ are the coordinates of the impact point of the two photons in the transverse plane.

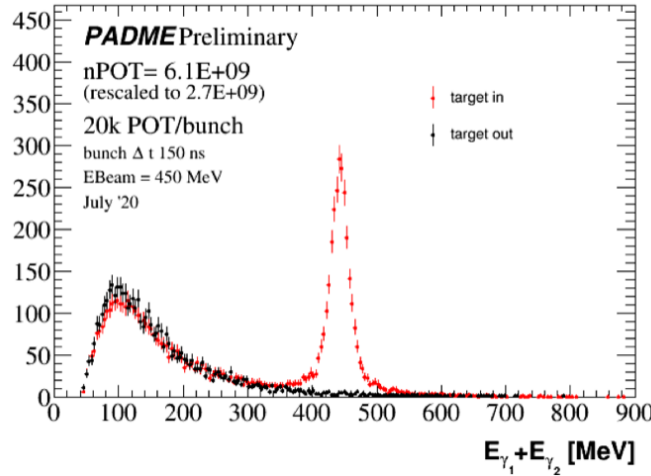


Figure 6: Sum of the energy of the two photons after the two-photon annihilation selection with and without target.

Starting from these considerations, the annihilation selection requires: two photons in time within $|\Delta t| < 10$ ns (this is a very loose cut when considering that the temporal resolution of ECAL is of about 1.3 ns); the leading photon of the pair is required to be inside the radial fiducial region, needed to reject clusters badly reconstructed due to energy leakage; a cut CoG was applied $|x(y)_{CoG}| < 5$ cm. Figure 6 shows the sum of the energies of the two photons for events passing this selection for data collected with and without the target.

6. Future search in PADME

Although PADME was designed to search for the dark photon, it is also well suited to search other dark candidates such as ALPs, Dark Higgs, and the protophobic X_{17} boson.

6.1 ALPs

A solution to the strong CP violating problem can be represented by the existence of the QCD axion. Nowadays, several experimental investigation are ongoing to search an ultralight, invisible axion, that should act as the only phenomenologically viable realization of the QCD axion.

Axion Like Particles (ALPs) with a mass in the MeV energy range can be produced through the e^+e^- annihilation, and can be detected exploiting two detection techniques according to the following mass hierarchy: if $M_a < 2M_{DM}$, the ALP decays to 2γ or e^+e^- pair, visible decay. In this case, the ALP detection can be possible due to the presence of 3γ or a pair of e^+e^- plus a photon. If $M_a > 2M_{DM}$, the ALP decays to a pair of dark matter particles, or it will not decay in the case of long-lived ALP. These latest cases embody the so-called invisible decay and the signature corresponds to the presence of a photon and missing energy (alternatively missing momentum or mass according to the experimental technique). Figure 7 shows the limits in the MeV axion

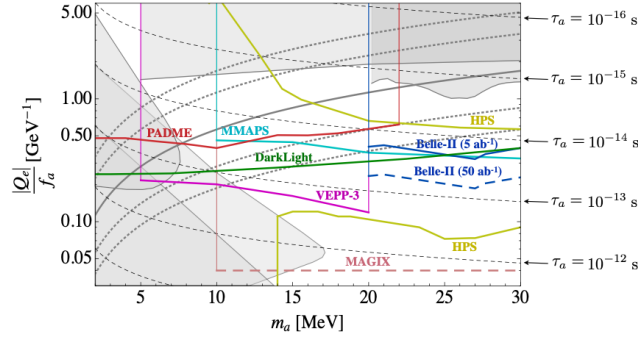


Figure 7: Projected reach of several planned dark photon experiments translated into the MeV axion parameter space, based on [151].

parameter space by translating the existing dark photon limits. Precisely, $\epsilon_{A'}$ can be mapped to the axion-electron coupling by the following relationship:

$$\epsilon_{A'}^2 \alpha \sim \frac{1}{4\pi} \left(\frac{Q_e}{f_a} m_e \right)^2 \quad (6)$$

where α is the fine-structure constant, f_a the coupling of the ALP particle, Q_e and m_e the charge and the mass of the electron, respectively.

Preliminary estimations of the number of ALPs produced in PADME for $\sim 10^{13}$ N_{POT} is about 1000 events for a mass equal to 22 MeV [15]. Deeper studies on ALP sensitivity for PADME is currently ongoing.

6.2 Dark Higgs

The decay mode of the dark Higgs depends on the mass hierarchy, indeed, if the relationship $m_{h'} \geq 2M'_A$ is satisfied, the dark Higgs will decay in two dark photons. In addition, if A' decays

in visible particles, $A' \rightarrow e^+e^-$, the dark Higgs can be discovered using the veto system with a multi-lepton time coincidence request. For a center of mass energy of $\sqrt{2m_e E_{beam}} \sim 22$ MeV, the dark Higgs production has a cross section not negligible with respect to the SM process $e^+e^- \rightarrow e^+e^-e^+e^-e^+e^-$ (which scales as $\epsilon^2 \times \alpha \times \alpha_{dark}$). More precisely:

- the cross section of the dark Higgs production is of the order of $\sigma(e^+e^- \rightarrow h'A' \rightarrow 3(e^+e^-)) \sim 1000$ pb;
- the cross section of the SM process that produce six leptons in the final state is $\sigma(e^+e^- \rightarrow 3(e^+e^-)) \sim 1500$ pb.

In this kind of search, a factor to consider is the acceptance of the experiment to observe six leptons. The studies of PADME sensitivity are ongoing.

6.3 Protophobic X_{17} boson

A possible discovery of a new particle has been claimed by the ATOMKI collaboration. The experiment measured electron-positron angular correlation for the 17.6 MeV and 18.15 MeV nuclear transitions in ${}^8\text{Be}$, observing an anomalous angular correlation. This anomaly can be interpreted as the creation and decay of an intermediate bosonic particle, the so-called X_{17} , with a mass of $m_X = 16.70 \pm 0.35(stat) \pm 0.5(sys)$ MeV [17]. In 2021, the collaboration observed a second anomaly in ${}^4\text{He}$ transitions, which can be explained by a similar resonance of similar mass $m_X = 17.00 \pm 0.13(stat) \pm 0.2(sys)$ MeV [18]. The collaboration asserts that the new particle is a boson with spin parity $J^P = 1^+$, which would couple to SM particles and, therefore, can be the mediator of a new force.

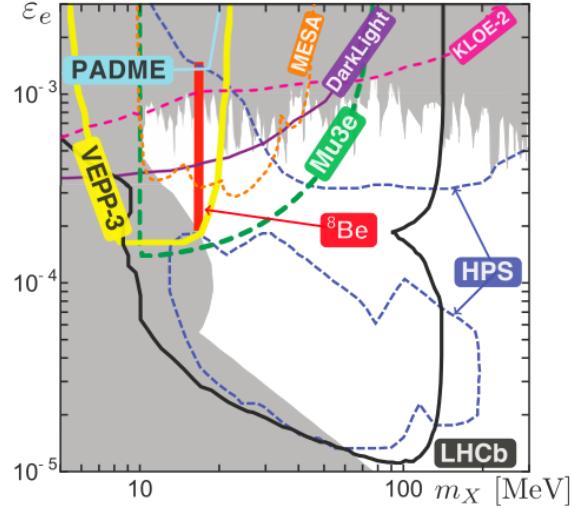


Figure 8: The ${}^8\text{Be}$ signal region of the ATOMKI experiment, along with the current constraints (gray) and projected sensitivities of future experiments in the (m_X, ϵ_e) plane [19].

Current and near future experiments will probe the parameter space of interest for the protophobic gauge boson X_{17} . Figure 8 shows the projected sensitivities of various experiments.

PADME can have a chance to confirm the existence of this new particle setting the positron beam energy to 282.7 MeV to exploit a resonant production [20]. The invariant mass of the charged lepton pair emerging from the target can be measured in PADME by means of the ECAL with a new charged particle tagger in front and turning off the magnetic field.

7. Conclusion

The PADME experiment uses for the first time a positron beam to search a dark photon produced in the annihilation with the electron of a fixed target. In this search, the missing mass technique is employed. During PADME RunI and RunII all detectors of the experiment performed according to the design expectation. A first analysis was accomplished of the main backgrounds for the dark photon, precisely two-photon annihilation and Bremsstrahlung. Although the main purpose is to search for the dark photon, the experiment can easily be adapted to investigate other dark matter candidates, such as ALPs, dark Higgs, and a protophobic boson X_{17} .

References

- [1] H. An, M. Pospelov, J. Pradler, *Observing dark photon with dark matter detectors* (2014), arXiv:1401.8287.
- [2] S. Biswas, E. Gabrielli, M. Heikinheimo, B. Mele, *Higgs-boson production in association with a dark photon in $e+e-$ collisions* (2016), arXiv:1503.05836
- [3] J. Beacham, et al., *Physics Beyond Colliders at CERN: Beyond the Standard Model Working Group Report* (2020). arXiv:1901.09966.
- [4] P. Valente et al., *Linear Accelerator Test Facility at LNF Conceptual Design Report* (2016), arXiv:1603.05651.
- [5] F. Oliva , *Operation and performance of the active target of PADME* (2019), Nuclear Inst. and Methods in Physics Research, A 162354, <https://doi.org/10.1016/j.nima.2019.162354>.
- [6] I. Oceano , *The performance of the diamond active target of the PADME experiment* (2020), Journal of Instrumentation 15 C04045.
- [7] G. Piperno et al., *Characterisation and performance of the PADME electromagnetic calorimeter* (2020), Journal of Instrumentation, vol. 15.
- [8] A. Frankenthal et al., *Characterization and performance of PADME's Cherenkov-based small-angle calorimeter* (2019), Nuclear Instruments and Methods in Physics Research, vol. 919.
- [9] G. Georgiev et al., *The PADME tracking system* (2016), RAD Association Journal, DOI:10.21175/radj.2016.03.034.
- [10] M.Raggi, V. Kozhuharov, *Proposal to search for a dark photon in positron on target collisions at daφne linac*, Advances in High Energy Physics (2014) 1–14doi:10.1155/2014/959802.

- [11] A. Belyaev, N. D. Christensen, A. Pukhov, *Calchep 3.4 for collider physics within and beyond the standard model*, Computer Physics Communications 184 (7) (2013) 1729–1769. doi:10.1016/j.cpc.2013.01.014.
- [12] S. Agostinelli, et al., *Geant4—a simulation toolkit*, Nuclear Instruments and Methods in Physics Research Section A: Accelerators, Spectrometers, Detectors and Associated Equipment 506 (3) (2003) 250–303. doi:https://doi.org/10.1016/S0168-9002(03) 01368-8.
- [13] F. Oliva, *The PADME Active Diamond Target and Positron Bremsstrahlung Analysis* (2021), P.h.D. thesis.
- [14] P.A. Zyla et al., *Particle Data Group*, Prog. Theor. Exp. Phys. 2020, 083C01 (2020)
- [15] F. Giacchino, *A light dark matter portal: The axion-like particle* (2019), Frascati Phys. Ser., 69:206–211.
- [16] P. Ciafaloni, G. Martelli, M. Raggi, *Searching for dark sectors in multi lepton final state in e^+e^- collisions* (2020), arXiv:2012.04754.
- [17] A. J. Krasznahorkay et al, *Observation of Anomalous Internal Pair Creation in ^8Be : A Possible Indication of a Light, Neutral Boson* (2016), arXiv:1504.01527.
- [18] A. J. Krasznahorkay et al, *A new anomaly observed in $4^H e$ supports the existence of the hypothetical X_{17} particle* (2021), arXiv:2104.10075.
- [19] Jonathan L. Feng et al, *Particle Physics Models for the 17 MeV Anomaly in Beryllium Nuclear Decays* (2016), arXiv:1608.03591.
- [20] E. Nardi et al, *Resonant production of dark photons in positron beam dump experiments* (2018), Physical Review D, 97(9).